J Electroceram (2007) 18:243–250
DOI 10.1007/s10832-007-9066-x

Synthesis of fine Ca-doped $BaTiO_3$ powders by solid-state reaction method—Part I: Mechanical activation of starting materials

Sung-Soo Ryu · Sang-Kyun Lee · Dang-Hyok Yoon

Received: 26 May 2006 / Accepted: 30 January 2007 / Published online: 27 February 2007
© Springer Science + Business Media, LLC 2007

Abstract Fine $(Ba_{0.98}Ca_{0.02})_{1.002}TiO_3$ powders for high capacitance multilayer ceramic capacitors (MLCCs) application were synthesized by solid state reaction method. The effects of mechanochemical activation using high energy milling and the starting materials properties on the reaction temperature and on the final powder properties were investigated. Previous heavy milling of $BaCO_3$ and the adoption of fine, anatase-rich TiO_2 phase were effective in decreasing the reaction temperature and in increasing the tetragonality (=c/a). $BaCaTiO_3$ powders with a tetragonality of 1.0097, an average particle size of 213±43 nm and a specific surface area of 6.30 m^2/g were acquired after heat treatment at 985 °C for 2 h. MLCCs utilizing this developed powder showed superior dielectric and temperature characteristics to those with conventional, Ca-free $BaTiO_3$ powder.

Keywords Powder-solid state reaction · Dielectric properties · $BaTiO_3$ · Capacitors

S.-S. Ryu
Korea Institute of Ceramic Engineering and Technology,
Seoul 153-801, South Korea

S.-K. Lee
Samsung Electro-Mechanics Co., Suwon 442-743, South Korea

D.-H. Yoon (✉)
School of Materials Science and Engineering,
Yeungnam University,
Gyeongsan 712-749, South Korea
e-mail: dhyoon@ynu.ac.kr

1 Introduction

It has been recognized that multilayer ceramic capacitors (MLCCs) having X5R or X7R characteristics require a core-shell microstructure to attain the stable temperature dependency and voltage characteristics of dielectric constant (K) [1, 2]. The core-shell structure is comprised of a ferroelectric core region and a diffused paraelectric shell region which surrounds the core mainly with additive materials. On the other hand, fine $BaTiO_3$ powders of approximately 200 nm particle size with high tetragonality (=c/a) are required to manufacture very thin-layered MLCCs with large capacitance and small size to keep up with recent trends in consumer electronics such as miniaturization and multi-functionalization [3]. However, the reduction in particle size usually accompanies the decreases in K as well as tetragonality [4–6].

Most MLCCs are currently produced with nickel instead of expensive palladium inner electrodes for cost reasons, which requires sintering under reducing atmosphere. Nevertheless, sintering in a low oxygen pressure atmosphere generates problems such as low insulating resistance and poor reliability mainly due to the oxygen vacancies, although efforts have been made to overcome these drawbacks by doping transitional metal ions such as Co^{3+}, Fe^{3+} and Mn^{3+} [7]. Sakabe et al. recently reported that 200 nm-sized $BaTiO_3$ powders produced by a hydrolysis method with high K, stable temperature dependence and with high reliability could be obtained by doping of a small amount of calcium [8]. Moreover, they explained that the high K of a sintered body using these powders came from the interfacial stress due to the role of the grain boundary without any core-shell formation. Since the formation of core-shell structure is increasingly difficult with fine powders due to the small core region, this finding is very interesting.

Among many $BaTiO_3$ synthetic methods, solid-state reaction method is considered the most conventional and the economic due to the utilization of the calcination of starting materials, usually barium carbonate and titanium oxide, at temperatures higher than 1,200 °C [3, 9]. This method tends to produce a significant amount of agglomeration, poor chemical homogeneity and coarse particle size due to the heat treatment at high temperature [3]. With the help of recently available advanced milling facilities and very fine starting materials, however, a few researchers have synthesized 200 nm-sized $BaTiO_3$ by this method [9–14]. Since the solid-state reaction occurs at the contact points of dissimilar materials, highly homogenized fine starting materials are very important for decreasing the reaction temperature and synthesizing fine particles. In addition, a much higher reaction rate with the particles exposed to heavy milling can be expected than those without milling due to the mechanochemical activation caused by the mechanical stress.

To the best of the authors' knowledge, no report has yet been published on the synthesis of very fine, Ca-doped $BaTiO_3$ powders using a solid-state reaction method for thin-layered MLCC application. Therefore, we examined the mechanochemical effects on the formation of solid-state reacted, Ca-doped $BaTiO_3$ powders by modifying the characteristics of the starting materials using a high energy mill. The morphological evolution of starting materials during milling, the effects of the starting materials' condition on the characteristics of the final powder and the resultant tetragonality values are discussed in Part I, presented here. The rheological behaviors of aqueous slurries on milling, the effects of slurry properties on milling efficiency and the dispersion stability associated with the mixing of starting materials in terms of steric and electrostatic mechanism will be discussed later in Part II, separately.

2 Experimental procedure

Commercial $BaCO_3$ powders (Sakai Chemicals, Japan) with a specific surface area of 19 m^2/g, and $CaCO_3$ powders (Ube Industries, Japan) with a specific surface area of 30 m^2/g were used for starting materials. In order to check the size and phase effects of TiO_2, two different kinds of commercial powders were used: a relatively coarse, 70% rutile/30% anatase-phased TiO_2 powder (Ishihara Corp., Japan) with a specific surface area of 20 m^2/g, and a fine, 10% rutile/90% anatase-phased TiO_2 powders (SDK, Japan) with a specific surface area of 50 m^2/g. Only $BaCO_3$ had an average particle size larger than 200 nm with a needle-like shape, while the other starting materials showed very fine spherical-shaped morphologies as shown in Fig. 1.

Forty kilograms of $BaCO_3$ was milled for 20 h using a high energy mill (LME 4, Netzsch, Germany) with 0.65 mm-diameter ZrO_2 beads and a rotational speed of 1,600 rpm before formulation of the starting materials. This

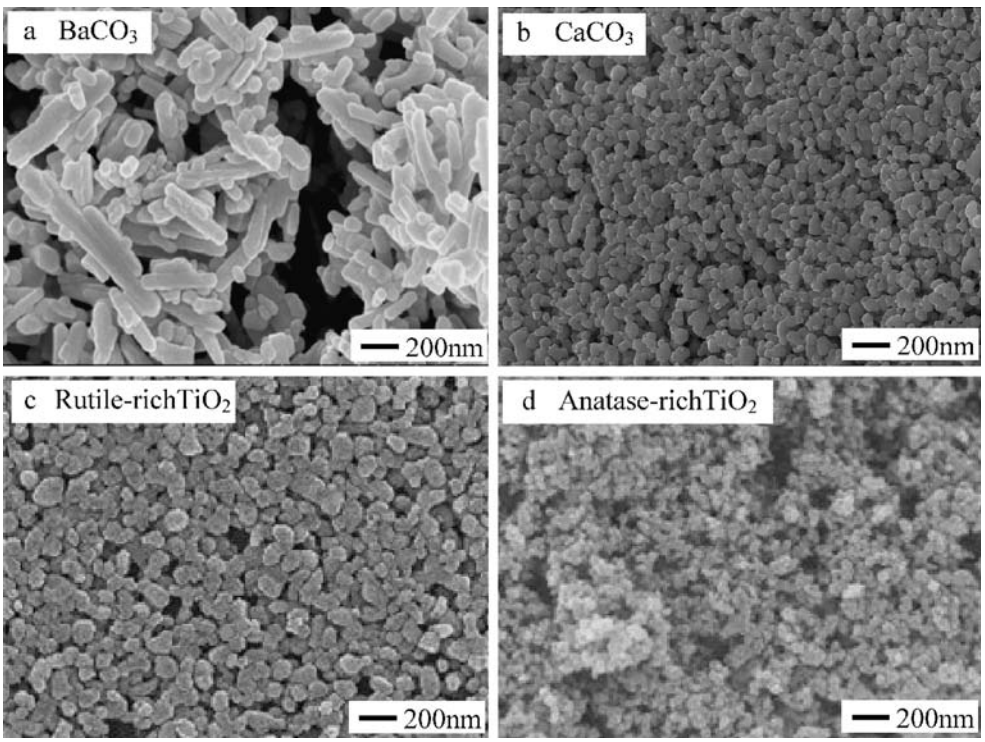

Fig. 1 SEM morphologies of starting materials

compound was previously milled because it showed the largest particle size and the most non-spherical shape. After drying and crushing of this milled $BaCO_3$ phase, three different kinds of formulation were performed depending on the combination of TiO_2 phases used and the $BaCO_3$ milling condition. The amounts of water adsorbed by the starting materials at room temperature were measured for each by heat treatment at 200 °C for 30 min. This temperature was set only for the measurement of physisorbed water in the powder to ensure the stoichiometry of the final powder by minimizing the weighing error, where the loss on ignition values ranged from 0.87 to 1.43 wt% depending on each starting material. The target formulation was $(Ba_{0.98}Ca_{0.02})_{1.002}TiO_3$ with a total batch size of 15 kg, where the relative molar ratios among the elements were checked and calibrated if needed during the experiments using an X-ray fluorescence (XRF, Simultix 12, Rigaku, Japan) technique. This large batch size was needed for the convenience of molar ratio adjustment and for MLCC manufacturing purpose. An ammonium salt of polycarboxylic acid (Cerasperse 5468-CF, San Nopco, Korea) was added as a dispersant, and de-ionized water with a conductivity lower than 1 μS/cm was used as liquid medium. A detailed description on the slurry formulation will be presented in Part II.

According to the type of TiO_2 used, two different types of powder were formulated: R-powder for the coarse, rutile-rich TiO_2 added one, and A-powder for the fine, anatase-rich TiO_2 added one. Both powder types contained previously milled $BaCO_3$ and a small amount of $CaCO_3$. A third powder, N-powder, was composed of $BaCO_3$ without previous milling, coarse, rutile-rich TiO_2 and $CaCO_3$. The three types of powders underwent an additional 8 h of milling, spray drying at 170 °C, pulverization and then heat treatment at various temperatures for 2 h in air at a heating rate of 7 °C/min. The powders were characterized using a scanning electron microscope (SEM: S-4100 using 10 kV with the working distance of 5–8 mm, Hitachi), X-ray diffractometer (XRD: RINT 2200 using Cu K_α line, Rigaku), thermo-gravimetric/differential thermal analyzer (TG/DTA: TGD 9600, TA Instruments), specific surface area measurement (BET: ASAP 2010 using N_2 adsorbent, Micromeritics) and particle size analyzer (PSA: LA-920 using laser scattering method, Horiba). Since PSA was not able to provide exact data on the primary particle size due to the necking and agglomeration of the powders, the average primary particle size was measured with SEM images for at least 100 particles simultaneously by using image analyzer software (SigmaScan, Systat Software, USA). X-ray diffraction (RINT 2200, Rigaku using Cu K_α line) patterns were utilized to determine the tetragonality of the final powders.

MLCCs of 1.5 μF capacitance were manufactured by adding Samsung's proprietary additives into A-powder, tape casting into 2.2 μm-thick green tapes and screen printing of the Ni inner electrode, etc. MLCCs with 180 active layers and a chip size of 1.0×0.5 mm were fired in a reducing atmosphere ($P_{O2}=1.5\times10^{-11}$ MPa at 1,156 °C). In

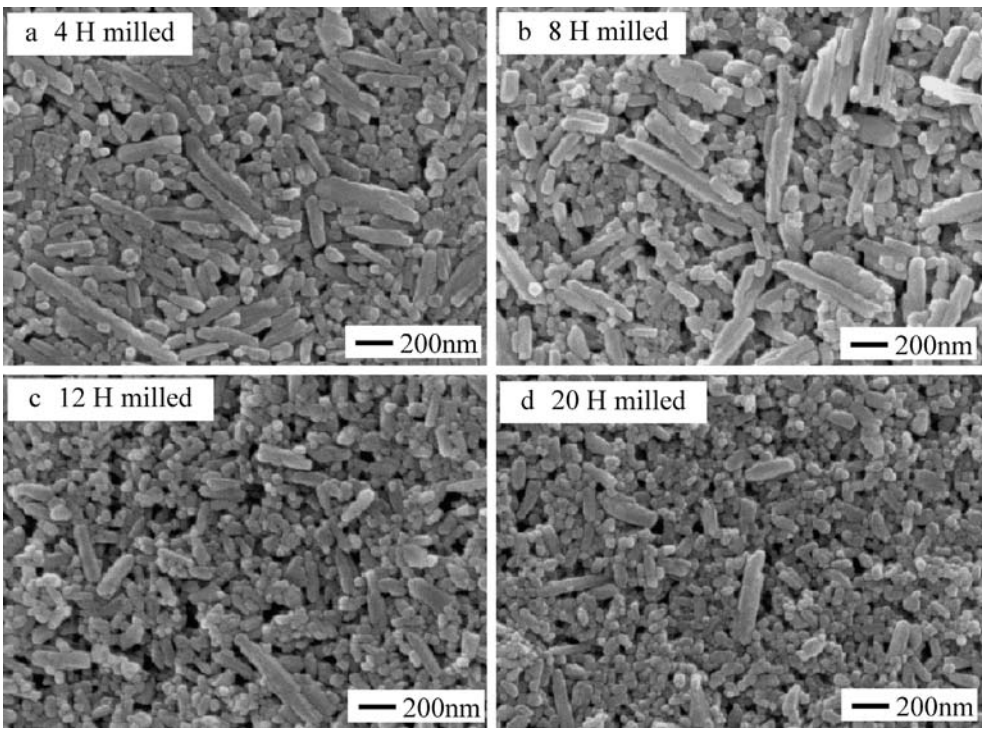

Fig. 2 Morphological changes of $BaCO_3$ as a function of high energy milling time

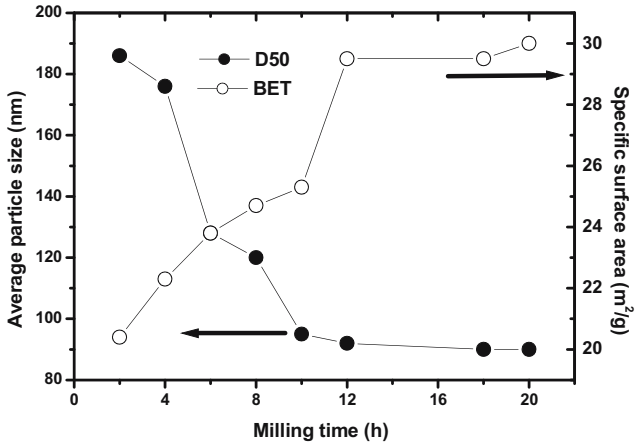

Fig. 3 Evolution of average particle size and specific surface area of $BaCO_3$ on milling

addition, small rectangular-shaped specimens, termed K^2s, were manufactured and fired at the same condition. The temperature coefficient of capacitance (TCC) and K at 85 °C of K^2s were measured by varying the applied electric field at 1 kHz using an LCR meter (HP-4284A) and a temperature control chamber. All of these properties were compared to the conventional powder without Ca-doping.

3 Results and discussion

Figure 2 represents the SEM images of the $BaCO_3$ particles during milling and shows a gradual decrease in the average particle size with increasing milling time. As shown in Fig. 1a, as-received powders had a coarse, needle-like shape with a broad particle size distribution. By considering the changes in average particle size measured by laser scattering method and in specific surface area over the 20-h milling time, as shown in Fig. 3, the initial surface area of 19 m^2/g evidently increased to 30 m^2/g while the average particle size decreased to less than 100 nm. The high milling efficiency represented by the drastic decrease in average particle size between 4 and 10 h of milling may be attributed to the rheological properties of the $BaCO_3$ slurry at this state, which will be explained later in Part II. Although a few needle-shaped particles remained after 20 h of milling, as shown in Fig. 2d, most of the $BaCO_3$ particles showed a significant decrease in particle size. The purpose of this milling was to obtain fine $BaCO_3$ particles in order to enhance the number of contact points of the starting materials.

The SEM images of the final formulation of A-powder during the additional 8 h of milling are shown in Fig. 4. Based on the SEM image of the 4-h-milled powder, which showed some needle-shaped $BaCO_3$ particles, as shown in Fig. 4a, an additional 4 h of milling was performed. The final starting materials before heat treatment had very fine particle sizes, as shown in Fig. 4b. Since drying using a vat may result in the layered segregation of the starting materials according to their relative densities, spray drying was performed with continuous stirring of the slurry. The resultant spherical-shaped granules had a diameter of 74.19± 12.31 μm.

TG/DTA results for the three different types of powders are shown in Fig. 5. Even though all three powders contained $CaCO_3$, most of the TG/DTA results were due to the effects of $BaCO_3$ and TiO_2 because the amount of $CaCO_3$ was very small. The weight loss between 600 and 900 °C corresponded to the $BaCO_3$ decomposition [13]. A-powder had a lower decomposition temperature than R- and N-powders, due to the effects of fine, anatase-rich TiO_2 phase and previous milling of $BaCO_3$. It has been reported that TiO_2 particles act as a catalyst for $BaCO_3$ decomposition [13, 15], and that the density of anatase phase is lower (3.90 g/cm^3) than that of rutile one (4.23 g/cm^3) [16]. These facts suggest that the fine anatase TiO_2 is more effective than the coarse rutile phase in decreasing the reaction temperature due to its large surface area and loose structure. According to the available thermodynamic data, the equilibrium temperature of $BaCO_3$ decomposition in air is about 820 °C in the absence of TiO_2 [17], but decreases to 640 °C for A-powder, as shown in Fig. 5. The effect of $BaCO_3$ milling on decreasing the reaction temperature was relatively smaller than that of fine anatase TiO_2, due to the decomposition temperature

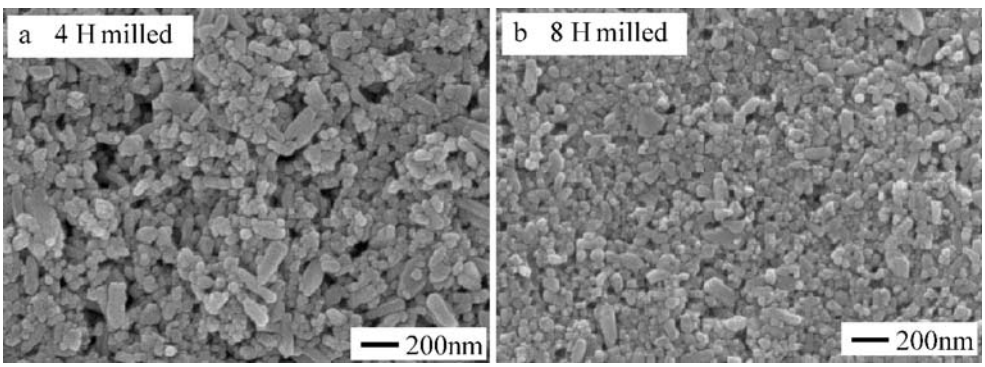

Fig. 4 SEM morphologies of A-powder containing the fine, anatase-rich TiO_2 phase: **a** 4-h and **b** 8-h milled powders

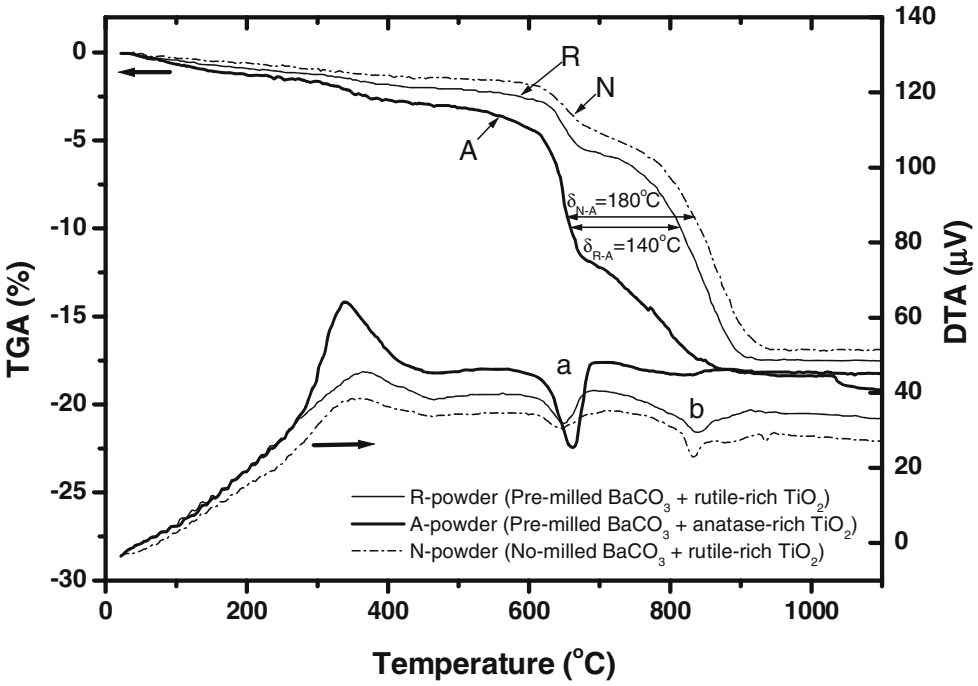

Fig. 5 Comparison of the TG/DTA results in air atmosphere with 3 °C/min heating rate for N-, R- and A-powders

differences among the three types of powder at this temperature range. The endothermic DTA peak near 640 °C (peak a) was from the decomposition of $BaCO_3$ while that of near 840 °C (peak b) was from the $BaCO_3$ phase transition from γ to β phase [13]. Since most of the $BaCO_3$ phase in A-powder was decomposed near 640 °C, the endothermic peak of this powder was large in this region while the peak due to the γ→β phase transition was insignificant compared to that of other powders.

$BaCaTiO_3$ phase started to appear from 900 °C for all three powders based on the XRD patterns after the heat treatment at various temperatures, as shown in Fig. 6. A-powder heat-treated at 900 °C was almost completely $BaCaTiO_3$ phase with a negligible amount of $BaCO_3$ phase, while both N- and R-powders still contained significant amount of starting materials at 900 °C due to the higher $BaCO_3$ decomposition temperature of these powders containing rutile-TiO_2 with a higher density than the anatase one, as shown in Fig. 5. The average particle size of A-powder was smaller than that of R- and N-powders for the 985 °C heat-treated samples, as shown by the SEM images in Fig. 7. The average particle sizes after 985 °C heat treatment were 241±63 nm, 235±54 nm, and 213±43 nm for N-, R-, and A-powders, respectively. Tetragonality values, the relative ratio of the lattice parameter of *c*- to *a*-axes (=*c*/*a*), of A-and R-powders as a function of the specific surface area at various heat treatment temperatures are shown in Fig. 8. A-powder with fine, anatase-rich TiO_2 phase showed a generally higher tetragonality than R-powder did at all temperatures in spite of its higher specific surface area, and hence the smaller particle size. For example, the 985 °C-heat treated A- and R-powders showed a tetragonality of 1.0097 and 1.0030, and average particle size of 213 and 235 nm and a specific surface area of 6.30 and 5.89 m^2/g, respectively. This finding is somewhat contradictory to our previous results which showed that the tetragonality of hydrothermal $BaTiO_3$ particles increased with increasing particle size [18]. This finding indicates that the tetragonality of $BaTiO_3$ or $BaCaTiO_3$ can be affected by the phase, particle size and processing conditions of the starting materials.

The reaction mechanism suggested by Beauger et al. [15] for the formation of $BaTiO_3$ by solid-state reaction is shown

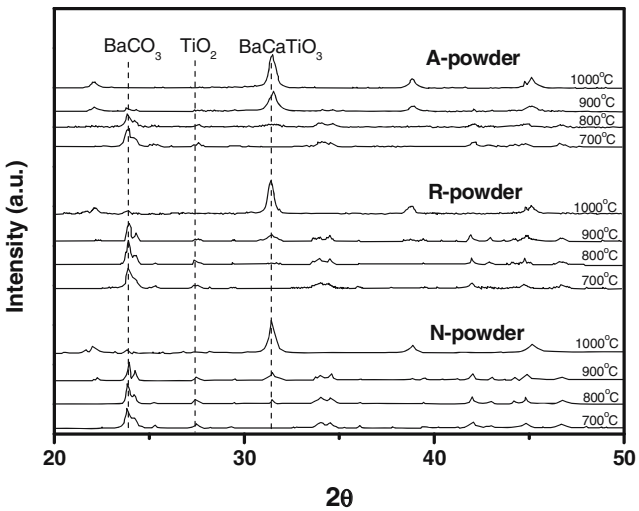

Fig. 6 XRD patterns of N-, R- and A-powders after heat treatment at various temperatures

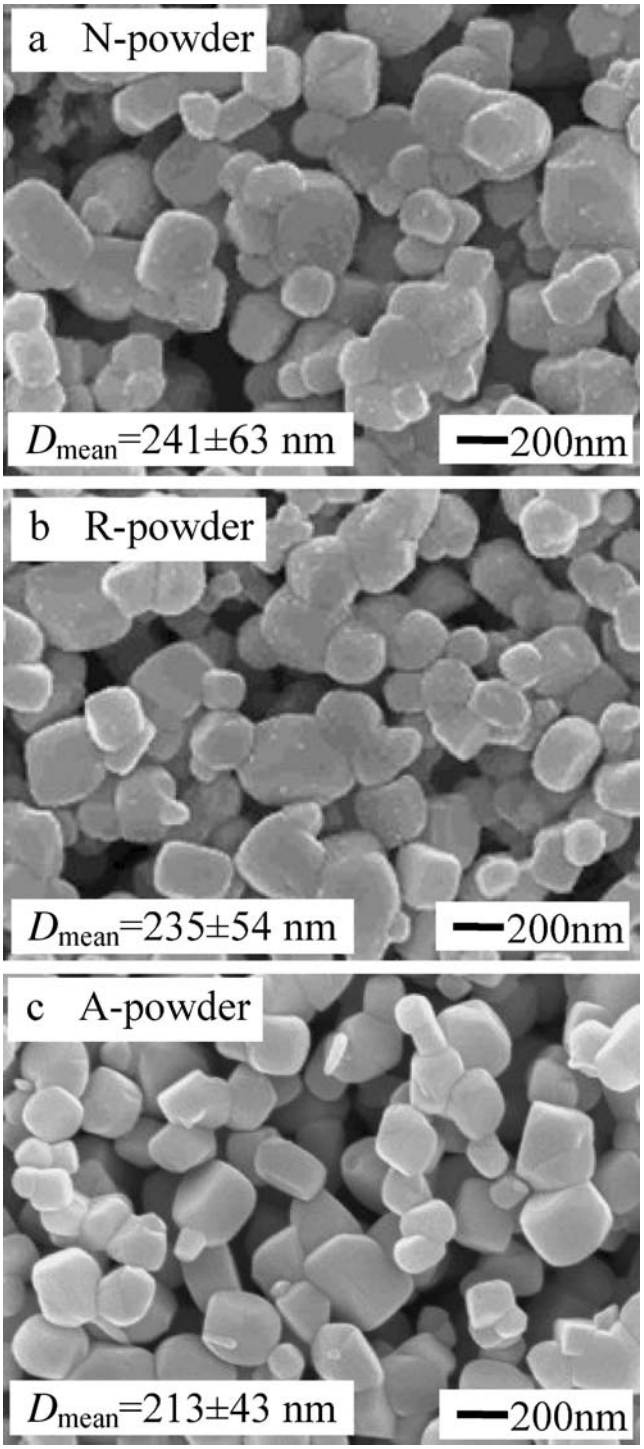

Fig. 7 SEM morphologies of **a** N-, **b** R- and **c** A-powders heat treated at 985 °C for 2 h. Average particle sizes measured using an image analyzer are shown

in the upper part of Fig. 9. According to this model, $BaTiO_3$ is easily formed at the surface of TiO_2 particles which also act as catalysts for $BaCO_3$ decomposition. When the surface $BaTiO_3$ layer is formed, the kinetics are governed by the barium and oxygen ion diffusion through this layer into the virgin TiO_2 phase. Due to the excess of barium and oxygen ions at the surface layer, Ba_2TiO_4 phase is generally formed initially. Homogeneous $BaTiO_3$ particles are formed gradually by the reaction between Ba_2TiO_4 and TiO_2 due to the continuous diffusion. This multi-step reaction mechanism is schematized in the lower part of Fig. 9, and can be applied for the formation of $BaCaTiO_3$. Consideration of this reaction mechanism suggest that the finer anatase-TiO_2 phase with looser and less dense structure than the rutile-TiO_2 phase may enhance the $BaTiO_3$ formation rate by decreasing both the diffusion length and activation energy, which is consistent with our findings. Moreover, very fine $BaCO_3$ particles may be helpful in this respect by increasing the contact points with other starting materials and by themselves undergoing easy decomposition.

According to Han et al. [19], Ca^{2+} prefers to occupy Ba-sites when (Ba+Ca)<Ti, but Ca^{2+} can be forced to occupy Ti-sites up to 2 mol% for (Ba+Ca)>Ti. Therefore, some Ti^{4+} sites must be replaced by a certain amount of Ca^{2+} for our experimental system, where the (Ba+Ca)/Ti ratio is 1.002, by generating oxygen vacancies according to the following equation:

$$CaO_{TiO_2} \rightarrow Ca''_{Ti} + O_O + V_O^{\bullet\bullet}$$

The occupation of Ti-sites by doped calcium ions increases the insulation resistance and reliability of MLCCs by decreasing the mobility of oxygen vacancies, even though the concentration of oxygen vacancies is increased, compared to Ca-free $BaTiO_3$, according to Sakabe et al. [8]. They also attributed the low mobility of oxygen vacancies to the lattice shrinkage caused by the replacement of barium ions by the remaining calcium ions with their smaller ionic radius.

Figure 10 compares (a) K and (b) TCC at 85 °C between the K^2s made from A-powder and the conventional Ca-free powder after adding Samsung's proprietary additives. K^2s with A-powder demonstrated reasonably high K of 3,000 at

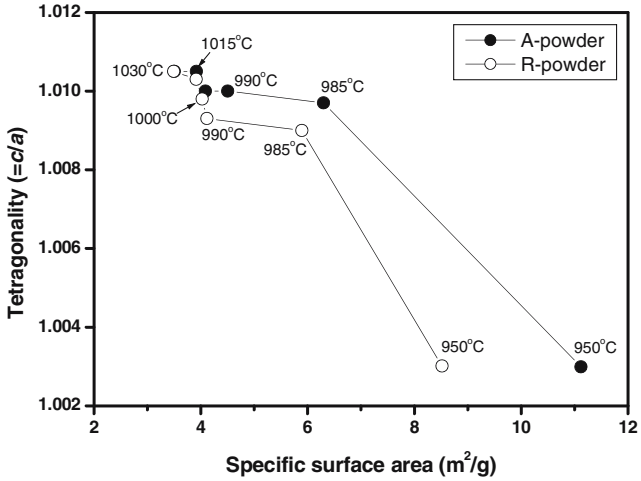

Fig. 8 Tetragonality values of A- and R-powders as a function of the specific surface area. Heat treatment temperatures are shown

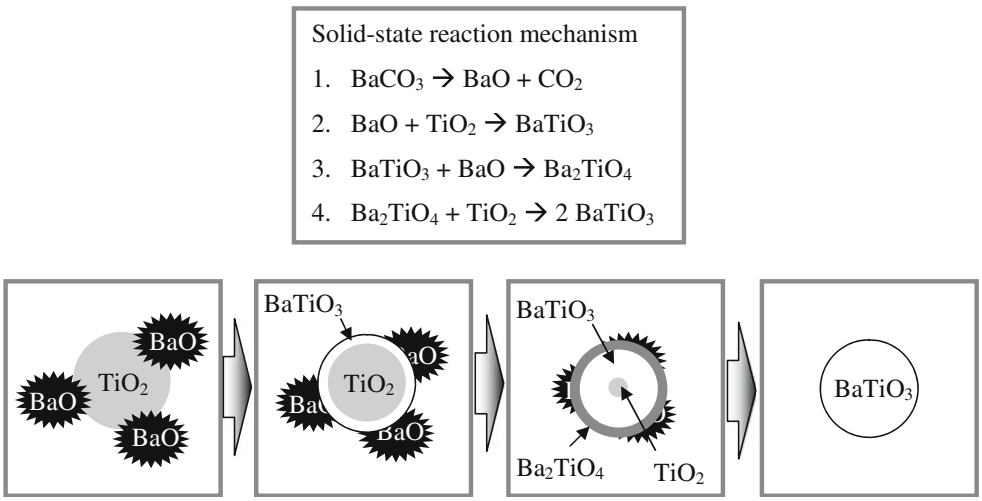

Fig. 9 Suggested solid-state reaction equation (*upper*) and a schematic model (*lower*) for the formation of $BaTiO_3$ from $BaCO_3$ and TiO_2

an AC field of 0.2 V/μm and stable TCC at 80 °C. Both of properties were superior to the Ca-free composition and can be applicable for high capacitance X5R MLCC with very thin dielectric layers. Since the direct measurement of dielectric properties of layers of approximately 1 μm thickness is impossible, varying the applied electric field using K^2 is a useful technique to predict the properties of thin dielectric layers. Moreover, both the dielectric layers and electrodes of MLCC showed quite dense morphologies, as represented in Fig. 10c.

4 Conclusion

The following conclusions were made based on the synthesis of fine $(Ba_{0.98}Ca_{0.02})_{1.002}TiO_3$ powders for high capacitance MLCC application by solid state reaction:

1. Fine $BaCaTiO_3$ powders with an average particle size of 213±43 nm and a specific surface area of 6.30 m^2/g were synthesized after heat treatment at 985 °C for 2 h in air atmosphere.

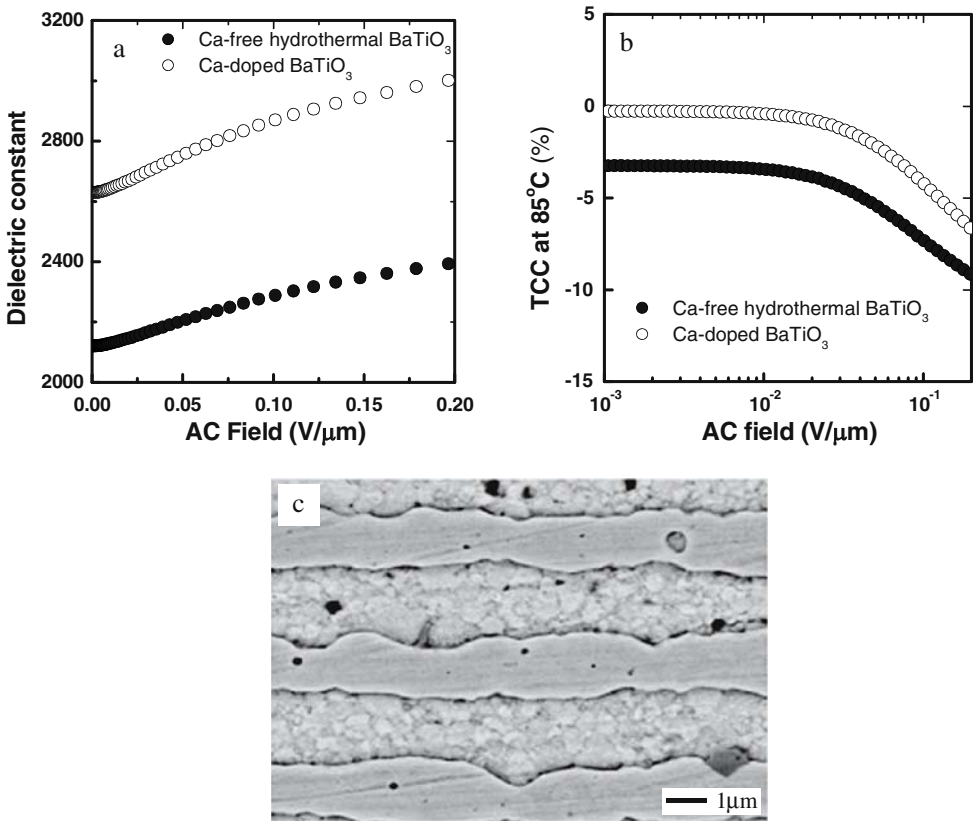

Fig. 10 Comparison of **a** dielectric constant behavior and **b** temperature coefficient of capacitance, at 85 °C between the K^2s made from A-powder and the conventional Ca-free powder, **c** SEM microstructure of MLCC manufactured using A-powder

2. Mechanochemical activation of starting materials by high energy milling and the adoption of fine, anatase-rich TiO_2 rather than coarse, rutile-rich phase were effective in decreasing the reaction temperature. Moreover, the particles produced under these conditions showed a higher tetragonality (=c/a) of 1.0097 than any other powders heat treated at the same temperature, despite their small particle size.
3. MLCCs manufactured using the developed powder showed higher dielectric constant (K) and more stable temperature characteristics than those using a Ca-free $BaTiO_3$ powder.

Acknowledgements The authors thank Dr. K. H. Hur, Mr. H. S. Jung and Mr. D. S. Lee at Samsung Electro-Mechanics Co. for their considerable cooperation.

References

1. Y. Park, H.G. Kim, J. Am. Ceram. Soc. **80**, 106 (1997)
2. H. Kishi, Y. Mizuno, H. Chazono, Jpn. J. Appl. Phys. **42**, 1 (2003)
3. D.H. Yoon, B.I. Lee, J. Ceram Process. Res. **3**(2), 41 (2002)
4. K. Uchino, E. Sadanaga, T. Hirose, J. Am. Ceram. Soc. **72**(8), 1555 (1989)
5. B.D. Begg, E.R. Vance, J. Nowotny, J. Am. Ceram. Soc. **77**(12), 3186 (1994)
6. R. Vivekanandan, T.R.N. Kutty, Powder Technol. **57**, 181 (1989)
7. M.T. Buscaglia, V. Buscaglia, V. Viviani, P. Nanni, M. Hanuskova, J. Eur. Ceram. Soc. **20**, 1997 (2000)
8. Y. Sakabe, N. Wada, T. Hiramatsu, T. Tonogaki, Jpn. J. Appl. Phys. **41**, 6922 (2002)
9. L.B. Kong, J. Ma, H. Huang, R.F. Zhang, W.X. Que, J. Alloys Compd. **337**, 226 (2002)
10. C. Gomez-Yanez, C. Benitez, H. Balmori-Ramirez, Ceram. Int. **26**, 271 (2000)
11. E. Brzozowski, M.S. Castro, J. Eur. Ceram. Soc. **20**, 2347 (2000)
12. V. Berbenni, A. Marini, G. Bruni, Thermochim. Acta **374**, 151 (2001)
13. E. Brzozowski, M.S. Castro, Thermochim. Acta **398**, 123 (2003)
14. C. Ando, R. Yanagawa, H. Chazono, H. Kishi, M. Senna, J. Mater. Res. **19**(12), 3592 (2004)
15. A. Beauger, J. C. Mutin, J. C. Niepce, J. Mater. Sci. **18**, 3543 (1983)
16. M.J. O'Neil, A. Smith, P.E. Heckelman, J.R. Obenchain, J.A.R. Gallipeau, M.A.D'Arecca, S. Budavari, *The Merck Index* (Merck, Whitehouse Station, NJ, 2001), p. 9549
17. I. Barin, *Thermochemical Data of Pure Substances: Part I* (VCH, Germany, 1989), p. 133
18. S.W. Kwon, D.H. Yoon, J. Eur. Ceram. Soc. **27**, 247 (2007)
19. Y.H. Han, J.B. Appleby, D.M. Smyth, J. Am. Ceram. Soc. **70**(2), 96 (1987)